



Formation of disinfection byproducts in an ammonia-polluted source water with UV/chlorine treatment followed by post-chlorination: A pilot-scale study

Xinran Zhang^{a,b}, Pengfei Ren^{c,*}, Jianhua Zhou^c, Junyi Li^c, Zhenxing Li^c, Ding Wang^d

^a Key Laboratory of Groundwater Resources and Environment (Jilin University), Ministry of Education, Changchun 130021, China

^b School of Environmental Science and Engineering, Guangdong Provincial Key Laboratory of Environmental Pollution Control and Remediation Technology, Sun Yat-sen University, Guangzhou 510001, China

^c Guangzhou Municipal Engineering Design & Research Institute, Guangzhou 510001, China

^d General Institute of Water Resources and Hydropower Planning and Design, Beijing, 100120, China

ARTICLE INFO

Article history:

Received 21 July 2021

Received in revised form 8 November 2021

Accepted 30 December 2021

Available online 4 January 2022

Keywords:

Disinfection byproduct

UV/chlorine treatment

Post-chlorination

NOM properties

Parallel factor analysis (PARAFAC)

ABSTRACT

This study investigated the formation of disinfection byproducts (DBPs) from a real ammonia-polluted source water treated by a pilot-scale ultraviolet (UV)/chlorine process with subsequent post-chlorination. The experimental results indicated that UV/chlorine treatment enhanced the formation of trihalomethanes (THMs), haloacetic acids (HAAs), and haloacetonitriles (HANs) in post-chlorination, compared to UV or chlorine applied alone under parallel experimental conditions. DBP formation was observed to depend on pH values, chlorine doses, and reaction times. THM formation was higher at pH 9.0 than pH 6.0, while HAAs and HANs were produced more readily at pH 6.0 rather than 9.0. A higher chlorine dose led to a higher amount of DBPs formed after the treatment of UV/chlorine followed by post-chlorination. The concentration of DBPs increased with the UV/chlorine treatment time increasing from 2 to 15 s and then presented a decrease trend with the reaction time prolonging to 30 s. In addition, changes in natural organic matter (NOM) properties were evaluated using three-dimensional fluorescence spectra and parallel factor analysis (PARAFAC) UV/chlorine treatment effectively destroyed humic-like and tyrosine-like components in waters with the maximum fluorescence intensity (FI_{max}) reduced by 51.4% and 64.6%, respectively, compared to the raw water sample. The decrease of fluorescence of waters exhibited a positive correlation with the formation of DBP-FP in UV/chlorine treatment. Overall, DBP formation from the ammonia-polluted source water caused by UV/chlorine treatment could be managed by carefully determining chlorine doses and contact times to be used in the UV/chlorine process.

© 2021 Published by Elsevier B.V. This is an open access article under the CC BY-NC-ND license (<http://creativecommons.org/licenses/by-nc-nd/4.0/>).

1. Introduction

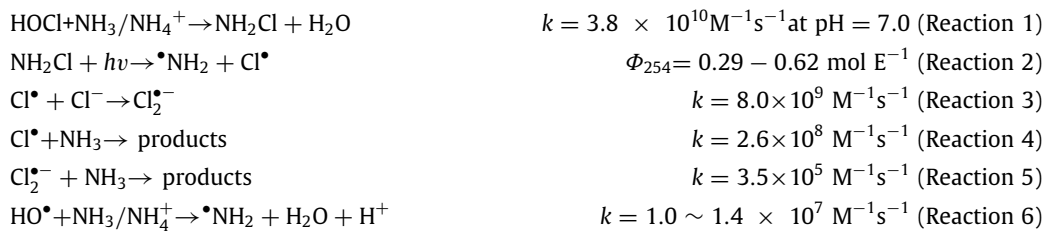
In recent years, the existence of ammonia in source water have been important issues of concern for drinking water supplies (Zhang et al., 2015). Ammonia is commonly observed in natural waters at concentrations ranging from

* Corresponding author.

E-mail address: pengfeiren84@163.com (P. Ren).

0.1 to 3 mg L⁻¹ and even as high as 10 mg L⁻¹ (Zhang et al., 2013). Ammonia reacts with free chlorine quickly in chlorination disinfection and form chloramines (mono-, di-, and tri-chloramine), as shown in Reaction 1. Excessive formation of chloramines is undesired since chloramines are weak disinfectants compared to free chlorine leading to inefficient disinfection. Moreover, the formation of disinfection byproduct (DBP) in ammonia containing waters is one of the major concerns. Ammonia enhanced the formation of nitrogenous-DBPs (N-DBPs), such as haloacetonitriles (HANs), haloacetamides (HAcAms), and halonitromethanes (HNMs) (Li and Mitch, 2018; Nihemaiti et al., 2017; Richardson et al., 2007). N-DBPs were reported to be highly toxic with cytotoxic and genotoxic levels one to two orders of magnitude higher than the regulated carbonaceous-DBPs (C-DBPs) (Villanueva et al., 2014; Chen et al., 2021).

Integrated application of UV irradiation and free chlorine (termed UV/chlorine) has emerged in recent years, showing promising potential to eliminate ammonia (Zhang et al., 2015). In UV/chlorine process, photolyzed chlorine generates hydroxyl radicals (HO•) and reactive chlorine species (RCS) (e.g., Cl•, Cl₂^{•-}, and ClO•) reacting with organic micro-pollutants (Wang et al., 2020; Kong et al., 2020; Wu et al., 2019b; Zhang et al., 2019a). Ammonia removal during the UV/chlorine treatment involves two pathways, i.e., photolysis of chloramines (Zhang et al., 2015) and radical-mediated oxidation of ammonia by hydroxyl radicals and reactive chlorine species (RCS) (Zhang et al., 2019b). The dominant reactions are listed in Reactions 1–6 (Zhang et al., 2019b; Wu et al., 2017).



Although UV/chlorine shows high efficiency in contaminant removal, it is concerned due to DBP formation. Specifically, natural organic matter (NOM) reacts with both free chlorine ($k_{\text{chlorine-NOM}} = 0.7\text{--}5 \text{ M}^{-1} \text{ s}^{-1}$) (Westerhoff et al., 2004) and reactive species ($k_{\text{NOM-HO}^\bullet} = 2.5 \times 10^4 \text{ (mg C L}^{-1}\text{)}^{-1} \text{ s}^{-1}$, $k_{\text{NOM-Cl}^\bullet} = 1.3 \times 10^4 \text{ (mg C L}^{-1}\text{)}^{-1} \text{ s}^{-1}$, and $k_{\text{NOM-ClO}^\bullet} = 4.5 \times 10^4 \text{ (mg C L}^{-1}\text{)}^{-1} \text{ s}^{-1}$) (Fang et al., 2014; Guo et al., 2017; Mertens and von Sonntag, 1995; Lei et al., 2020). In particular, aromatic and aliphatic components of NOM are preferentially targeted by HO• and RCS through either hydrogen abstraction or hydroxylation (Varanasi et al., 2018). RCS also induces transformation of olefins and amine groups via addition, electron transfer, and H-abstraction (Guo et al., 2017). As a result, the concentration of NOM-induced DBPs formed during the UV/chlorine treatment could be higher than the level during chlorination alone (Lei et al., 2021). Moreover, the reactions between these reactive species and NOM may also produce more DBP precursors, which further promotes DBP formation during the UV/chlorine treatment as well as the following post-chlorination process.

However, the UV/chlorine treatment at full-scale drinking water treatment plants enhanced DBP formation potential for trihalomethanes (THMs), haloacetic acids (HAAs), adsorbable organic halogen (AOX) and total organic halogen (TOX), compared with chlorination alone (Wang et al., 2015, 2019). The degradation of NOM by UV/chlorine treatment has been found to generate more HAAs, HANs and HALs relative to chlorination alone (Wang et al., 2017; Gao et al., 2019). Whereas, another study reported that the UV/chlorine treatment slightly decreased the formation of trichloromethane (TCM) and trichloroacetic acid (TCAA) in a humic acid solution (Li et al., 2016). Our previous investigation suggested that UV/chlorine generated less THMs and HAAs compared with breakpoint chlorination when treating ammoniacal water, while the formation of HANs for UV/chlorine was approximately twice of that for breakpoint chlorination (Zhang et al., 2015). The discrepancy of DBP formation could be caused by various water quality and the experimental conditions. It is therefore necessary to evaluate DBP formation in real ammonia-polluted water treated by UV/chlorine.

Although DBP formation in the UV/chlorine process has received some investigation, it is far away from complete understanding. Many bench-scale studies exist for the formation of DBPs in the UV/chlorine process using the synthetic water, but few studies have been carried out using a real ammonia-polluted source water in a pilot-scale. The relationship between NOM and DBP formation has not been well examined. Therefore, more fundamental research is required to investigate the resultant DBP formation due to UV/chlorine treatment especially in an actual ammonia-polluted source water at larger scale (e.g., in a pilot-scale setting).

This study aims to contribute to a better understanding of DBP formation. A real ammonia-polluted source water was treated in a pilot-scale UV/chlorine advanced oxidation system followed by a post-chlorination process. The formation of a wide range of C-DBPs and N-DBPs were analyzed. The effects of pH, chlorine doses, and UV/chlorine treatment times were also assessed. Transformation of NOM structures during the UV/chlorine treatment was subsequently evaluated using fluorescence spectroscopy. Based on the observations, the linkages between DBP formation and NOM transformation were found and discussed.

2. Materials and methods

2.1. Water quality and chemicals

Water to be used was from a drinking water treatment plant in northeastern China. Important water quality parameters are shown in Table 1 with moderate dissolved organic carbon ($4.26 \pm 0.10 \text{ mg C L}^{-1}$) and nitrate ($4.75 \pm 0.05 \text{ mg N L}^{-1}$)

Table 1
Water quality parameters of the tested water.

Parameter	Value	Parameter	Value
DOC (mgC·L ⁻¹)	4.26 ± 0.10	SUVA (L·mg ⁻¹ ·m ⁻¹)	3.02 ± 0.01
NH ₄ ⁺ (mgN·L ⁻¹)	0.92 ± 0.05	NO ₃ ⁻ (mgN·L ⁻¹)	4.75 ± 0.05
NO ₂ ⁻ (mgN·L ⁻¹)	N.D.	TON (mgN·L ⁻¹)	0.16 ± 0.02
Cl ⁻ (mg·L ⁻¹)	47.3 ± 0.8	Br ⁻ (mg·L ⁻¹)	N.D.
pH	7.5 ± 0.1	Alkalinity (mg·CaCO ₃ L ⁻¹)	113.5 ± 3.0

Note: N.D. means no detectable.

levels and a high ammonia nitrogen concentration (0.92 ± 0.05 mg N L⁻¹). Sodium hypochlorite solutions (NaOCl, 10% active chlorine by weight), sodium sulfite, sodium hydrogen phosphate, and sodium dihydrogen phosphate were obtained from J&K Scientific (Beijing, China). Standard solutions for THMs, HAAs, and HANs were purchased from Sigma-Aldrich (USA). The other reagents were reagent grade or higher and obtained from the Aladdin Industrial Corporation (Beijing, China). The experimental solutions were prepared with water produced by a Milli-Q purification system. Free chlorine stock solutions at 1000 mg L⁻¹ as Cl₂ were prepared using a commercially available NaOCl solution and stored in the dark at 4 °C.

2.2. Experimental procedures

Pilot-scale experiments were conducted using a continuous flow-through UV reactor (volume: 1.8 L, length: 35 cm, stainless steel) centered with a 17 W low-pressure UV lamp emitting 254 nm UV light. This reactor was illustrated in our previous paper (Zhang et al., 2015). An incident UV fluence rate of 1.0×10^{-2} W cm⁻² determined using the iodide-iodate actinometry method (Rahn et al., 2006). When varied fluence rates were required in some tests, the water flowrate was adjusted to reach appropriate contact times ranging from 5 to 30 s, which corresponded to UV doses of 50–300 mJ cm⁻². In each trial, the water to be treated was pumped through an inlet of the reactor and collected at the outlet. An injection valve upstream of the UV lamp was used to add free chlorine at a given dose no more than 4.0 mg L⁻¹ as Cl₂. By switching this valve and the UV lamp on and off, the water could be treated by UV irradiation, chlorination, UV/chlorine, or nothing as a control. When using the UV lamp, it was warmed for 20 min in advance to ensure a constant output.

The experiments were conducted at pH 6.0, pH 7.5 and pH 9.0 to investigate the effects of pH on DBP formation. The pH condition was adjusted using sulfuric acid (H₂SO₄) and sodium hydroxide (NaOH) solutions. No pH buffer was added. Chlorine residual after the UV/chlorine treatment and chlorination alone was 0.8 and 1.2 mg L⁻¹ as Cl₂, respectively. Since chlorine dose is an important factor influencing DBP formation, a uniform post-chlorination condition was applied. The residual chlorine after pre-treatment was completely quenched and added a given dose of chlorine (10 mg L⁻¹) for post-chlorination in all cases. After 30 min, 24 h and 72 h of post-chlorination, the concentrations of residual chlorine were 3.5, 1.1 and 0.2 mg L⁻¹ as Cl₂, respectively. Chlorine residual was then quenched by sodium sulfite (Na₂SO₃) at an excess concentration three folds as high as the chlorine concentration. It should be noted that adding Na₂SO₃ was found to have a minimal effect (less than 0.5%) on the degradation of DBPs. All the tests were conducted in triplicate with a relative standard deviation (RSD) for each triplicate set of less than 5% to meet quality assurance/quality control (QA/QC) requirements. The standard deviations are illustrated as error bars in the figures shown afterwards.

2.3. Analytical methods

DBP samples with a volume of 30 mL were extracted by adding 3 mL of methyl *tert*-butyl ether (MTBE) containing 1, 2-dibromopropane as a surrogate standard and 6 g oven-dried anhydrous sodium sulfate. The concentrations of THMs, HAAs, HANs, chloral hydrate (CH), trichloropropanone (TCP), and trichloronitromethane (TCNM) were then determined using a gas chromatograph (Agilent 7890 A) coupled with an electron capture detector (ECD). A HP-5 fused silica capillary column (30 m × 0.25 mm I.D. with a 0.25 mm film thickness, J&W Scientific) was operated according to the following temperature protocol: a hold at 35 °C for 9 min, a ramp to 40 °C at 2 °C min⁻¹, then another ramp to 160 °C at 20 °C min⁻¹, and a final hold at 160 °C for 10 min. The method detection limits (MDLs) for these DBPs were determined to be 0.01–0.2 µg L⁻¹.

Free chlorine was measured using N,N-diethyl-p-phenylene diamine (DPD)/ferrous titration (APHA, 2005). DOC was identified using a Shimadzu TOC-V_{CPH} analyzer. Ammonia concentrations were detected using a pH/ISE meter (Thermo Orion 720 A) equipped with an ammonia selective electrode (Thermo Orion 95-12) (APHA, 2005). The minimum reporting limit (MRL) of ammonia was 0.01 mg L⁻¹ as N. Fluorescence of NOM in water was characterized based on three-dimensional fluorescence spectra (excitation–emission matrix, EEM) generated by a fluorescence spectrophotometer (F-4500, Hitachi). The emission spectra were scanned in the range of 270 to 550 nm, and the excitation wavelengths were determined from 240 to 450 nm with an increment of 5 nm. The normalized EEM volume in a given region was calculated according to a previously established method (Yang et al., 2008). Parallel factor analysis (PARAFAC) was performed to analyze the EEM spectra using MATLAB 6.0 and the DOMFluor toolbox (Mangalgi et al., 2021; Cai et al., 2020, 2017; Lee et al., 2018)

3. Results and discussion

3.1. DBP formation promoted by uv, chlorination, and UV/chlorine treatment

The concentrations of dominant DBPs (i.e., THMs, HAAs, and HANs) formed during UV irradiation, chlorination, and UV/chlorine followed by post-chlorination were shown in Figs. 1 and 2. DBP concentration in all tests without post-chlorination was undetectable. Two post-chlorination time were performed because that 30 min of post-chlorination is a typical disinfection time at drinking water treatment plants in China, while 72 h reaction time was applied to unveil DBP formation potential (DBP-FP) that could be reached in a distribution network. Noted that the raw waters contained a relatively high ammonia nitrogen ($0.92 \pm 0.05 \text{ mg N L}^{-1}$), chlorine reacted with ammonia quickly and converted to monochloramine. Herein, “UV/chlorine” referred to the mixed process of UV/chlorine and UV/chloramine. Additionally, the “blank” samples in Figs. 1 and 2 were defined as the samples without any pre-treatment before directly exposure to post-chlorination.

3.1.1. THMs and HAAs

Fig. 1a shows the formation of THMs in tested water treated by UV irradiation, chlorination, or UV/chlorine for 15 s with subsequent post-chlorination for 30 min (the left section) and 72 h (the right section). It can be seen that UV alone led to minimal THM formation during the 30 min post-chlorination (approximately $2.0 \mu\text{g L}^{-1}$), while UV/chlorine resulted in the concentration of THMs formed during 30 min post-chlorination (6.2 to $7.1 \mu\text{g L}^{-1}$) even slightly lower than that pretreated by chlorine alone (7.3 to $8.6 \mu\text{g L}^{-1}$). This result was consistent with a previous study reporting that UV/chlorine did not immediately increase the formation of THMs in NOM water compared to chlorination alone (Wang et al., 2017). However, with a longer post-chlorination time (72 h), the THM formation potential (THM-FP) pretreated by UV/chlorine was enhanced obviously compared to that pretreated by chlorine alone. Compared to the water pretreated by UV alone, chlorination increased THM-FP by 25.6–28.6%, while UV/chlorine made an extra 22.2–42.8% increase from the level with chlorination, leading to a concentration of 56.7 – $63.6 \mu\text{g L}^{-1}$. Additionally, the formation of HAAs was similar with THMs formation, as shown in Fig. 1b. UV/chlorine pretreatment caused lower HAA formation compared to that pretreated by chlorination, whereas UV/chlorine brought about a level of HAA formation potential (HAA-FP) 27.4–58.8% higher than that with chlorination pretreatment.

The results of carbonaceous disinfection by-products (C-DBPs, including THM and HAA) formation indicated that the UV/chlorine treatment imposed a very limited impact on the formation of DBPs during a short post-chlorination period (for 30 min). Whereas, it significantly increased formation potential of C-DBP during a relatively long post-chlorination process (for 72 h). This obvious enhancement in UV/chlorine may be attributed to more C-DBP precursors formation during the UV/chlorine treatment than that during chlorination alone. Alternatively, it may be because UV/chlorine promotes the efficiency of the conversion of DBP precursors in post-chlorination. The mechanistic reason will be discussed later in Section 3.4 through analysis of NOM moieties.

3.1.2. HANs

Fig. 2 displays a trace level of HAN formation ($< 0.8 \mu\text{g L}^{-1}$) during 30 min post-chlorination with pretreatment of UV, chlorine, and UV/chlorine, while the concentration was much higher after the water underwent a long post-chlorination reaction for 72 h. To be specific, HAN formation potential (HAN-FP) associated with UV irradiation was 5.9 – $7.4 \mu\text{g L}^{-1}$, and the value for chlorination was 11.8 – $13.2 \mu\text{g L}^{-1}$. Similar to THM and HAA formation potentials, UV/chlorine made HAN-FP greatly enhanced to a level of 14.5 – $21.8 \mu\text{g L}^{-1}$. The significant rise in HAN-FP by UV/chlorine was consistent with a recent study reporting an obvious increase in dichloroacetonitrile (DCAN) formation in water containing 0.5 mg L^{-1} ammonia exposed to 300 mJ cm^{-2} UV and 72 h post-chlorination (Zi et al., 2018).

The great enhancement of HAN-FP in the UV/chlorine treatment was likely associated with relatively high contents of nitrogenous matters in the raw water. As shown in Reaction 1, free chlorine (3.0 mg L^{-1} as Cl_2) quickly reacts with ammonia (0.92 mg N L^{-1}) to form monochloramine (NH_2Cl), with a reaction rate constant of $3.1 \times 10^6 \text{ M}^{-1} \text{ s}^{-1}$ (Pressley et al., 1972). NH_2Cl has been identified as a N-DBP precursor (Yang et al., 2010). It has been found that the enhanced DCAN formation in the ammoniacal water received UV irradiation and post-chlorination, suggesting ammonia can serve as a DCAN precursor (Zi et al., 2018). In addition, organic chloramines can also form N-DBPs by producing aldehyde intermediates during the UV/chlorine treatment, which will subsequently convert to HAN (Shah and Mitch, 2011). Besides, UV irradiation leads to photolysis of inorganic/organic chloramines and generates reactive nitrogen species (RNS, including $\bullet\text{NH}_2$, $\bullet\text{NH}_2\text{O}_2$, $\bullet\text{NO}$, and NO_2^\bullet), as illustrated in Reactions 2 and 7–9 (Pagsberg, 1972; Laszlo et al., 1998; Mack and Bolton, 1999). UV photolysis of chloramine derivatives promotes the involvement of RNS in the formation of N-DBP precursors, which were then oxidized and transformed to N-DBPs during post-chlorination. (Ruan et al., 2021; Zhou et al., 2020).



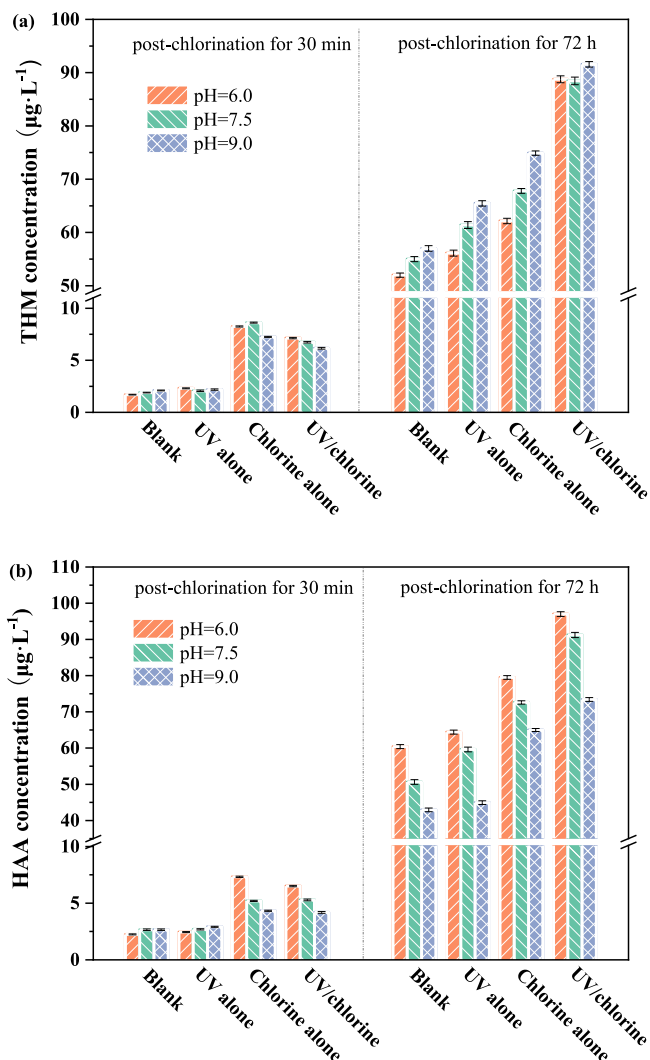


Fig. 1. THMs (a) and HAAs (b) formed in different treatment processes followed by 30 min or 72 h of post-chlorination. Conditions: $[\text{chlorine}]_0 = 3.0 \text{ mg L}^{-1}$ as Cl_2 , UV dose = 150 mJ cm^{-2} ; pH = 6.0, 7.5 and 9.0; free chlorine concentration in post-chlorination = 10 mg L^{-1} .

3.2. Impact of pH on the formation of thms, haas, and hans

In addition to the results discussed above, Figs. 1 and 2 also illustrate the impact of pH on DBP formation in the UV/chlorine treated real water. THMs, HAAs, and HANs at pH 6.0, 7.5, and 9.0 were analyzed after the water was treated by UV, chlorine, and UV/chlorine with/without subsequent post-chlorination. In general, similar pH effects were observed on both short-term DBP formation (for 30 min post-chlorination) and long-term formation potential (for 72 h post-chlorination). THMs increased as the pH rose from 6.0 to 9.0, suggesting that an alkaline condition was beneficial for the formation of THMs. In contrast, the highest formation of HAAs and HANs was found at 6.0. In addition, it is interesting that the pH effects were more obvious in the water pretreated by UV/chlorine as compared to chlorination pretreatment. This implied that the formation of DBPs in both UV/chlorine and chlorination processes likely obey similar pathways, but UV/chlorine facilitated the formation of more DBP precursors than the latter.

The dependence of DBP formation on pH involved complicated reactions. As mentioned above, under the experimental conditions, monochloramine (NH_2Cl) formed immediately after adding 3.0 mg L^{-1} free chlorine to water with 0.92 mg N L^{-1} ammonia. It has been known that the photolysis rate of NH_2Cl under UV irradiation at pH 6.0 is quicker than that at pH 9.0 (Yin et al., 2020). An acidic pH condition also facilitates the conversion of NH_2Cl to dichloramine (NHCl_2), a more photosensitive compound than NH_2Cl via an acid-catalyzed disproportionation pathway (Valentine et al., 1986). Furthermore, an alkaline condition associates with a higher concentration of hydroxyl ions (HO^-), which is a strong RCS scavenger reacting with Cl^\bullet and $\text{Cl}_2^{\bullet-}$ fast (rate constants: 1.8×10^{10} and $4.5 \times 10^7 \text{ M}^{-1}\text{s}^{-1}$, respectively) (Zhang et al.,

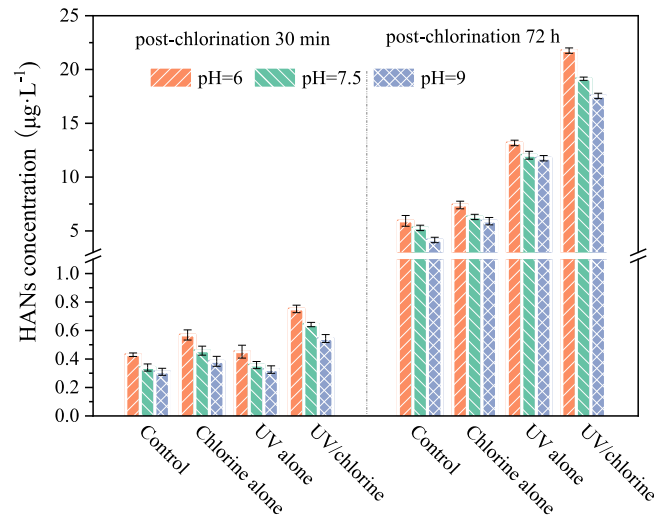


Fig. 2. HANs formed in different treatment processes followed by 30 min or 72 h of post-chlorination. Conditions: $[\text{chlorine}]_0 = 3.0 \text{ mg L}^{-1}$ as Cl_2 , UV dose = 150 mJ cm^{-2} ; pH = 6.0, 7.5 and 9.0; free chlorine concentration in post-chlorination = 10 mg L^{-1} .

2019b; Chuang et al., 2017). As a result, higher concentrations of HO^\bullet , RCS, and reactive nitrogen species (RNS) occurred at a lower pH, thereby facilitating the formation of DBP precursors. On the other hand, free chlorine attacked DBP precursors faster at a lower pH value during the post-chlorination period. HAA formation peaked at pH 6.0, partially reflecting more HAA precursors formed at pH 6.0 than pH 7.5 and 9.0. In terms of HANs, the lower formation at a higher pH largely resulted from lower stability of HANs in an alkaline environment via a base-catalyzed hydrolysis process (Hong et al., 2017; Fang et al., 2010). Since pH has different effects on the formation of THMs, HAAs and HANs, total cytotoxicity of the DBPs after 72 h of post-chlorination was assessed as an overall indicator of the pH impact. The cytotoxicity was calculated by using the concentrations of detected DBPs divided by their lethal concentration to 50% (LC50) values determined using CHO cells (Wagner and Plewa, 2017). The calculated cytotoxicity values of the DBPs formed during the UV/chlorine process were 2.7 to 2.8 times of those treated by chlorine alone at pH 6.0, 7.5 and 9.0. The cytotoxicity values for 72 h of post-chlorination at these three pH values were 0.0036, 0.0032 and 0.0029, respectively. HANs contributed to more than 90% of the total cytotoxicity, primarily due to the high cytotoxicity of DCAN. It can be seen that an alkaline condition leads to a lower DBP cytotoxicity value.

3.3. Impact of UV/chlorine operational conditions on the formation of DBPs

3.3.1. Impact of chlorine dosages

Fig. 3 shows DBP formation due to UV/chlorine treatment at various chlorine doses ($1\text{--}4 \text{ mg L}^{-1}$) followed by post-chlorination with 10 mg L^{-1} free chlorine for 24 h. This test simulated the condition in a typical clear well at a potable water treatment plant. Two THMs (chloroform (TCM) and bromodichloromethane (BDCM)), two HAAs (dichloroacetic acid (DCAA) and trichloroacetic acid (TCAA)), two HANs (dichloroacetoneitrile (DCAN) and trichloroacetoneitrile (TCAN)), as well as chloralhydrate (CH), trichloro-2-propanone (TCP), and trichloronitromethane (TCNM), were detectable, whereas other regular DBPs were lower than detection limits. It can be seen in Fig. 3 that the total concentrations of DBPs increased with an increase in the chlorine dose. Among these DBPs, TCM and TCAA increased more significantly than others. When the chlorine dosage increased from 1.0 to 4.0 mg L^{-1} , the concentration of TCM increased by 221% and the concentration of TCAA increased by 256%. As to nitrogenous disinfection by-products (N-DBPs), increasing chlorine dosage from 1.0 to 4.0 mg L^{-1} , led to the concentration of DCAN slightly increased from 3.2 µg L^{-1} to 4.2 µg L^{-1} . Overall, these results suggested that the increase in the chlorine dosage enhances DBPs formation and their precursors. A higher chlorine dose results in higher radical levels that produces more DBP precursors (Wang et al., 2017). Therefore, limiting chlorine dosages to a reasonable level is probably a good way to control DBPs during the UV/chlorine treatment.

3.3.2. Impact of UV/chlorine reaction times

Fig. 4 shows the impact of UV/chlorine treatment times on the formation of DBPs. The total concentration of DBPs reached the maximum (78.9 µg L^{-1}) at 15 s of UV/chlorine followed by 24 h of post-chlorination, and then, the total DBPs concentration slightly reduced to 72.3 µg L^{-1} when the UV/chlorine time extended to 30 s. The results suggested that when a prolonged UV/chlorine reaction time was applied, the formation of C-DBPs, including TCM, BDCM, DCAA, and TCAA, increased first and then decreased slightly during the following post-chlorination process. The highest C-DBPs concentration was achieved with a reaction time of 15 s. As opposed to C-DBPs, the concentrations of N-DBPs, such

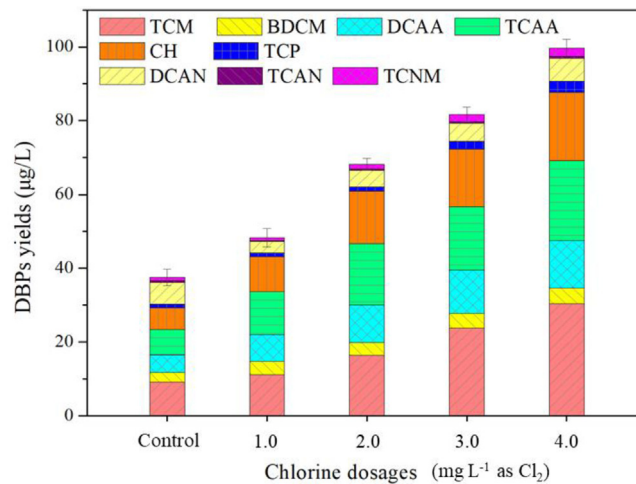


Fig. 3. DBP formation from micro-polluted water in UV/chlorine treatment followed by 24 h post-chlorination under different chlorine dosages. Condition: UV fluence = 150 mJ cm^{-2} , pH = 7.5; free chlorine concentration in post-chlorination = 10 mg L^{-1} .

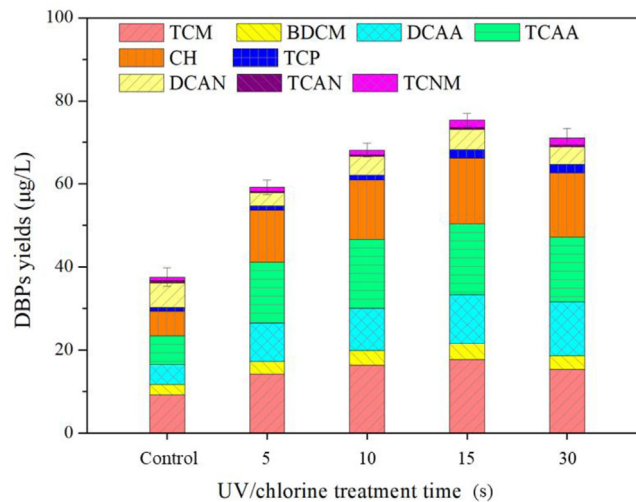


Fig. 4. DBP formation from micro-polluted water in UV/chlorine treatment followed by 24 h post-chlorination under different UV/chlorine reaction times. Conditions $[\text{chlorine}]_0 = 3 \text{ mg L}^{-1}$, UV fluence = $50\text{--}300 \text{ mJ cm}^{-2}$, pH = 7.5; free chlorine concentration in post-chlorination = 10 mg L^{-1} .

as DCAN and TCAN, changed slightly regardless with UV irradiation time varying from 5 to 30 s. The reason for these results is that NOM in the water was partially oxidized to aldehydes and ketones (as important DBPs precursors) and then further oxidized to carboxylic acids with a longer UV reaction time (Wang et al., 2017). However, further increasing the UV/chlorine treatment time could destroy parts of DBP precursors to some extent. Under the experimental conditions of this study, the impacts of UV/chlorine treatment time on DBP formation are not as significant as the chlorine dosages. Additionally, post-chlorination time also affected the DBPs formation potential. Under the same UV/chlorine treatment time (15 s), the DBP yields after 30 min, 24 h and 72 h of post-chlorination were 12.7 , 78.9 and 198.8 µg L^{-1} , respectively, indicating that DBP formation potential increased with a longer post-chlorination time.

3.4. Changes in NOM molecules influencing DBP formation during the UV/chlorine treatment

Fig. 5 shows three-dimensional fluorescence spectra of the raw water and the samples treated by UV irradiation, chlorination, and UV/chlorine without post-chlorination. The excitation–emission matrix (EEM) spectroscopy shows two identifiable peak regions: Ex/Em: $280\text{--}320/420\text{--}460 \text{ nm}$ and Ex/Em: $230\text{--}260/420\text{--}460 \text{ nm}$, corresponding to humic-like and fulvic acid-like substances, respectively. The results demonstrate that UV alone made a negligible change in the fluorescence spectra of NOM. Therefore, direct photolysis did not contribute to NOM transformation. A notable reduction in the fluorescence intensities was observed in the samples chlorinated or UV/chlorine treated, agreeing with the results

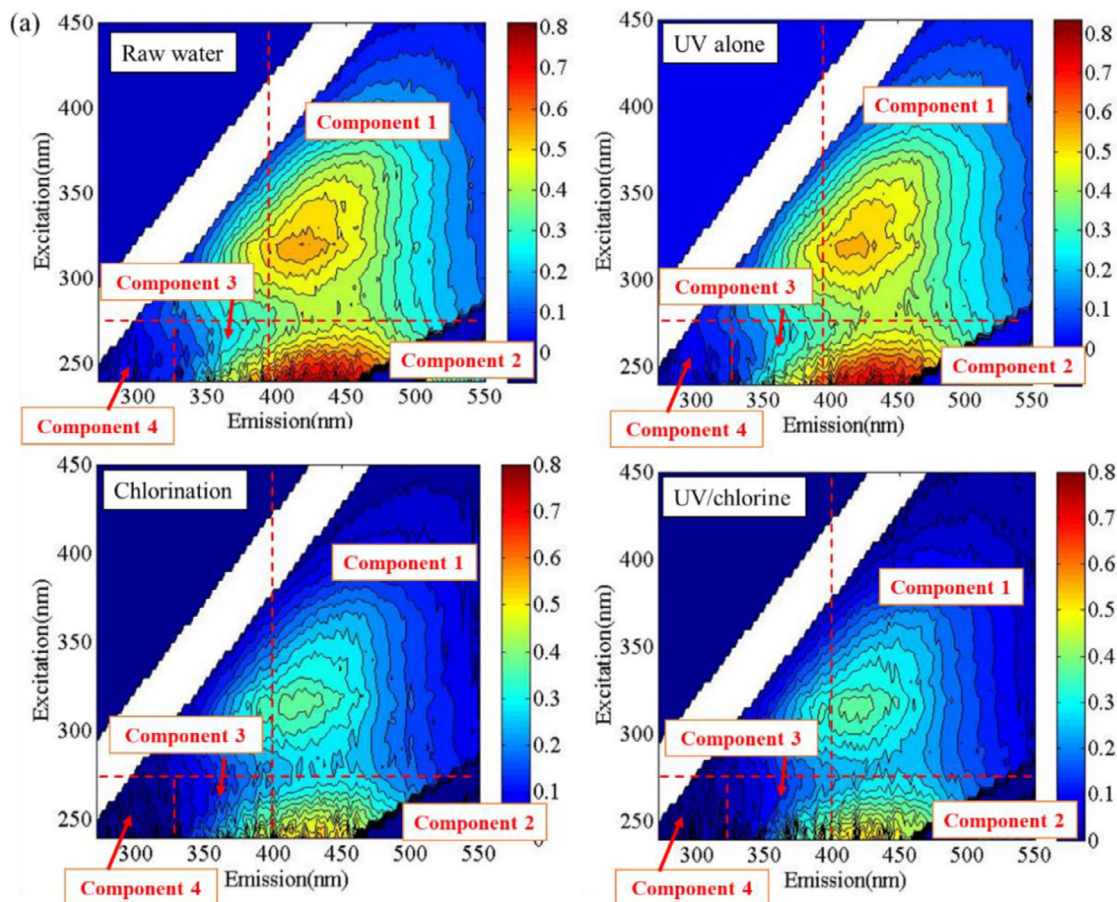


Fig. 5. EEM spectra of samples after UV irradiation, chlorination, and UV/chlorine treatment. Conditions: [chlorine] = 3.0 mg L⁻¹ as Cl₂, UV dose = 150 mJ cm⁻², pH = 7.5.

reported a previous study (Meng et al., 2013). Furthermore, the fluorescence intensity decreasing after the UV/chlorine treatment was more obvious than that after the chlorination, suggesting that the UV/chlorine treatment destroyed NOM chromophore more effectively than chlorine alone. Since direct photolysis only affected the NOM transformation slightly (as evidenced by the results from the UV alone tests), the indirect degradation of NOM by reactive radicals and free chlorine during the UV/chlorine treatment was the main reason leading to the destruction of chromophore and fluorophore structures of the NOM molecules.

Parallel factor analysis (PARAFAC) distinguished four fluorescence components of the EEM spectra including hydrophobic humic-like (C1, Ex/Em: 260-370/470), fulvic-like (C2, Ex/Em: 250/420), microbial humic-like (C3, Ex/Em: 310/370), and protein-like (C4, Ex/Em: 290/320) groups. The results are shown in Fig. 6a. Maximum fluorescence intensity (FI_{max}) was applied to reflect the changes in each component due to treatment. As shown in Fig. 6b, C2 was predominant, followed by C1, C3, and C4. The results show that UV exposure contributed to minimal changes (less than 5%) in each component, which agree with the EEM spectra shown in Fig. 5. The UV/chlorine treatment was found to remove each component more efficiently than chlorination. Specifically, in UV/chlorine treatment, FI_{max} values for C1, C2, C3 and C4 declined by 51.0%, 32.7%, 34.3% and 64.6%, respectively. Whereas, in chlorination alone, the FI_{max} values for C1, C2, C3 and C4 reduced by 40.4%, 24.0%, 29.5% and 53.9%, respectively. These results indicate the hydrophobic humic-like (C1) and tyrosine-like components (C4) were much more reactive in the UV/chlorine treatment than that of the fulvic-like and protein-like components.

In theory, the UV/chlorine treatment can destroy NOM molecules, such as unsaturated bonds and aromatic structures, through both photolysis and oxidation pathways initiated by radicals (Wols and Hofman-Caris, 2012). RCS preferentially attacks electron-rich moieties (such as unsaturated bonds, phenolic groups, and amines), causing NOM molecule breakdown. The reaction rate constants of NOM with HO[•], Cl[•], and ClO[•] are 2.5×10^4 , 1.3×10^4 , and 4.5×10^4 M⁻¹s⁻¹, respectively (Guo et al., 2017). The interactions between the electron donating moieties of NOM (e.g., unsaturated bonds and aromatic structures) and the reactive species (e.g., RCS) enhance DBP formation during the UV/chlorine treatment (Bulman and Remucal, 2020). Additionally, transformation of organic matter from a higher molecular weight

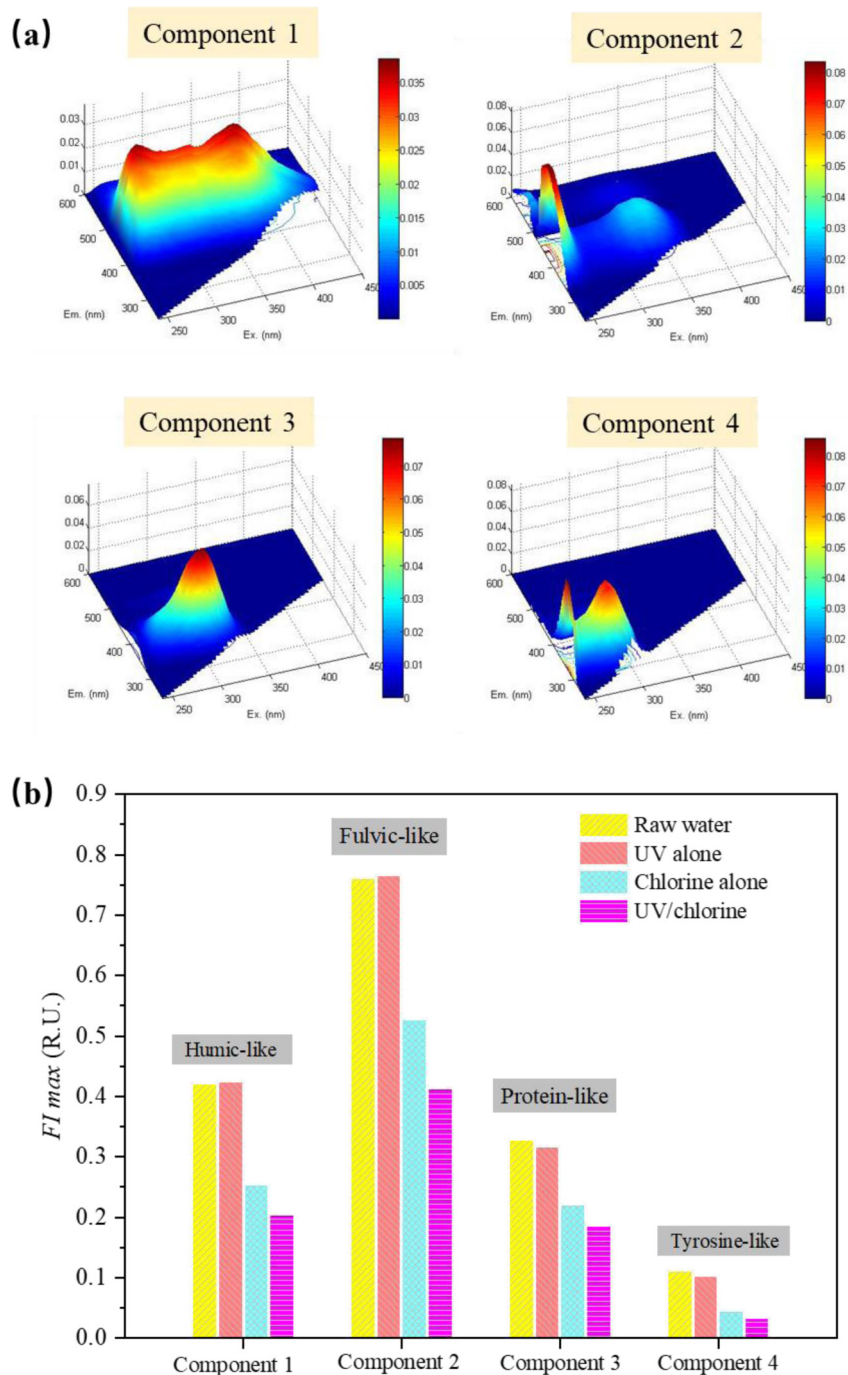


Fig. 6. (a) Surface plots of four components of water samples identified from the EEM datasets; (b) Maximum fluorescence intensity values of four components with UV, chlorine alone, and UV/chlorine treatment. Conditions: $[\text{chlorine}]_0 = 3.0 \text{ mg L}^{-1}$ as Cl_2 , UV dose = 150 mJ cm^{-2} .

to a lower molecular weight takes place during the UV/chlorine treatment, when a lot of intermediates are formed, which could be DBP precursors and convert to DBPs in post-chlorination (Li et al., 2016). As a result, the reactive radicals ($\text{HO}\cdot$, $\text{Cl}\cdot$, and others) alter NOM characteristics and increase its reactivity toward free chlorine, which brings about an increase in DBP formation during post-chlorination as observed in this study.

A positive correlation can be found between the enhanced removal of chromophore and fluorophore structures and the formation of DBP precursors. UV/chlorine treatment accelerated the destruction of C1, C2, C3 and C4 by 18.5%, 11.4%, 6.9% and 23.1%, respectively, compared to chlorine alone. These results indicate that $\text{HO}\cdot$ and RCS preferred to

consume tyrosine-like components in raw waters. However, compared to chlorine alone, UV/chlorine pre-treatment enhanced the formation of THMs, HAAs and HANs during 72 h post-chlorination by 30.5%, 25.7% and 59.2%, respectively. This was probably because HO^{*} and RCS degraded more chromophore and fluorescent components and produced more intermediates, which reacted with chlorine readily to form more DBPs during post-chlorination. Considering the intensity and the sensitivity of these four components, humic-like components (C1) and tyrosine-like components (C4) could be employed as indicators of C-DBP and N-DBP formation potentials, respectively. More investigation is needed to obtain better understanding of the relationships between chromophore components and DBP formation.

4. Conclusions and engineering implications

UV/chlorine followed by 30 min post-chlorination slightly affected the formation of DBPs compared to chlorination alone. However, UV/chlorine treatment greatly enhanced the formation potentials of all detectable DBPs after 72 h post-chlorination, compared to chlorination alone. The effects of pH were different in terms of different DBPs. More THMs were formed at pH 9 than at pH 6 during the UV/chlorine treatment, while an opposite trend was found for the formation of HAAs and HANs versus pH. A higher chlorine dose facilitated higher formation of DBPs during post-chlorination. The fluorescence analyzes demonstrated that the changes in specific components of the water samples shaped the subsequent DBP formation. The changes of chromophore and fluorescent present in water during UV/chlorine treatment may serve as a DBP-FP indicator, which need further investigation. Generally, the optimization of chlorine doses and UV irradiation time is important to control DBP formation in UV/chlorine process. Adjusting pH for DBPs control may not be a promising approach, because pH exhibits diverse effects on the formation of different DBPs.

Overall, the results contribute to better understanding of the UV/chlorine process before seeking practical applications. Compared to chlorine alone, the UV/chlorine process exhibited better performance on the removal of organics introduced from raw water, but increased the formation potential of DBPs. Besides organic DBPs, UV/chlorine process could cause the formation of bromate (a potential carcinogen) when the source water contains bromide (Aghdam et al., 2017; Hua et al., 2021; Yeom et al., 2021). It has been found a synergistic effect between organic DBPs and bromate, which enhanced the overall toxicity of DBPs produced (Han and Zhang, 2018; Wu et al., 2019a). More multidisciplinary and comprehensive studies on DBP formation and its toxicological consequences should be conducted to further assess the UV/chlorine process prior to practical use.

CRedit authorship contribution statement

Xinran Zhang: Investigation, Data curation, Writing – original draft. **Pengfei Ren:** Visualization, Writing – review & editing. **Jianhua Zhou:** Validation. **Junyi Li:** Investigation. **Zhenxing Li:** Investigation. **Ding Wang:** Supervision, Writing – review & editing.

Declaration of competing interest

The authors declare that they have no known competing financial interests or personal relationships that could have appeared to influence the work reported in this paper.

Acknowledgments

This study was supported by the Open Project Program of Key Laboratory of Groundwater Resources and Environment (Jilin University, China), Ministry of Education (grant number 202005007KF), National Science Foundation of China (grant number 51808156), the Guangdong Basic and Applied Research Foundation (2019A1515011664), the Fundamental Research Funds for the Central Universities (grant number 201gzd22).

References

- Aghdam, E., Xiang, Y.Y., Sun, J.L., Shang, C., Yang, X., Fang, J.Y., 2017. DBP formation from degradation of DEET and ibuprofen by UV/chlorine process and subsequent post-chlorination. *J. Environ. Sci-China* 58, 146–154.
- APHA, 2005. Standard Methods for the Examination of Water and Wastewater. American Public Health Association, Washington, DC, USA.
- Bulman, D.M., Remucal, C.K., 2020. Role of reactive halogen species in disinfection byproduct formation during chlorine photolysis. *Environ. Sci. Technol.* 54, 9629–9639.
- Cai, W., Han, J., Zhang, X., Liu, Y., 2020. Formation mechanisms of emerging organic contaminants during on-line membrane cleaning with NaOCl in MBR. *J. Hazard. Mater.* 386, 121966.
- Cai, W., Liu, J., Zhu, X., Zhang, X., Liu, Y., 2017. Fate of dissolved organic matter and byproducts generated from on-line chemical cleaning with sodium hypochlorite in MBR. *Chem. Eng. J.* 323, 233–242.
- Chen, C., Du, Y., Zhou, Y., Wu, Q., Zheng, S., Fang, J., 2021. Formation of nitro(so) and chlorinated products and toxicity alteration during the UV/monochloramine treatment of phenol. *Water Res.* 194, 116914.
- Chuang, Y.H., Chen, S., Chinn, C., Mitch, W.A., 2017. Comparing the UV/monochloramine and UV/free chlorine advanced oxidation processes (AOPs) to the UV/hydrogen peroxide AOP under scenarios relevant to potable reuse. *Environ. Sci. Technol.* 51, 13859–13868.
- Fang, J., Fu, Y., Shang, C., 2014. The roles of reactive species in micropollutant degradation in the UV/free chlorine system. *Environ. Sci. Technol.* 48, 1859–1868.

- Fang, J., Ma, J., Yang, X., Shang, C., 2010. Formation of carbonaceous and nitrogenous disinfection by-products from the chlorination of microcystis aeruginosa. *Water Res.* 44, 1934–1940.
- Gao, Z., Lin, Y., Xu, B., Xia, Y., Hu, C., Zhang, T., Cao, T., Chu, W., Gao, N., 2019. Effect of UV wavelength on humic acid degradation and disinfection by-product formation during the UV/chlorine process. *Water Res.* 154, 199–209.
- Guo, K., Wu, Z., Shang, C., Yao, B., Hou, S., Yang, X., Song, W., Fang, J., 2017. Radical chemistry and structural relationships of PPCP degradation by UV/chlorine treatment in simulated drinking water. *Environ. Sci. Technol.* 51, 10431–10439.
- Han, J., Zhang, X., 2018. Evaluating the comparative toxicity of DBP mixtures from different disinfection scenarios: a new approach by combining freeze-drying or rotoevaporation with a marine polychaete bioassay. *Environ. Sci. Technol.* 52 (18), 10552–10561.
- Hong, H., Yan, X., Song, X., Qin, Y., Sun, H., Lin, H., Chen, J., Liang, Y., 2017. Bromine incorporation into five DBP classes upon chlorination of water with extremely low SUVA values. *Sci. Total Environ.* 590–591, 720–728.
- Hua, Z., Li, D., Wu, Z., Wang, D., Cui, Y., Huang, X., Fang, J., An, T., 2021. DBP formation and toxicity alteration during UV/chlorine treatment of wastewater and the effects of ammonia and bromide. *Water Res.* 188, 116549.
- Kong, Q., Lei, X., Zhang, X., Cheng, S., Xu, C., Yang, B., Yang, X., 2020. The role of chlorine oxide radical (ClO center dot) in the degradation of polychloro-1, 3-butadienes in UV/chlorine treatment: kinetics and mechanisms. *Water Res.* 183.
- Laszlo, B., Alfassi, Z.B., Neta, P., Huie, R.E., 1998. Kinetics and mechanism of the reaction of $\cdot\text{NH}_2$ with O_2 in aqueous solutions. *J. Phys. Chem. A* 102, 8498–8504.
- Lee, D., Kwon, M., Ahn, Y., Jung, Y., Nam, S.-N., Choi, I.-h., Kang, J.-W., 2018. Characteristics of intracellular algogenic organic matter and its reactivity with hydroxyl radicals. *Water Res.* 144, 13–25.
- Lei, Y., Lei, X., Westerhoff, P., Zhang, X., Yang, X., 2021. Reactivity of chlorine radicals (Cl^\cdot and Cl_2^\cdot) with dissolved organic matter and the formation of chlorinated byproducts. *Environ. Sci. Technol.* 55, 689–699.
- Lei, X., Lei, Y., Zhang, X., Yang, X., 2020. Treating disinfection byproducts with UV or solar irradiation and in UV advanced oxidation processes: A review. *J. Hazard. Mater.* 124435.
- Li, T., Jiang, Y., An, X., Liu, H., Hu, C., Qu, J., 2016. Transformation of humic acid and halogenated byproduct formation in UV-chlorine processes. *Water Res.* 102, 421–427.
- Li, X.F., Mitch, W.A., 2018. Drinking water disinfection byproducts (DBPs) and human health effects: multidisciplinary challenges and opportunities. *Environ. Sci. Technol.* 52, 1681–1689.
- Mack, J., Bolton, J.R., 1999. Photochemistry of nitrite and nitrate in aqueous solution: a review. *J. Photochem. Photobiol. A* 128, 1–13.
- Mangalgi, K., Cheng, Z., Cervantes, S., Spencer, S., Liu, H., 2021. UV-based advanced oxidation of dissolved organic matter in reverse osmosis concentrate from a potable water reuse facility: A parallel-factor (PARAFAC) analysis approach. *Water Res.* 204, 117585.
- Meng, F., Huang, G., Yang, X., Li, Z., Li, J., Cao, J., Wang, Z., Sun, L., 2013. Identifying the sources and fate of anthropogenically impacted dissolved organic matter (DOM) in urbanized rivers. *Water Res.* 47, 5027–5039.
- Mertens, R., von Sonntag, C., 1995. Photolysis ($\lambda = 254\text{nm}$) of tetrachloroethene in aqueous solutions. *J. Photochem. Photobiol. A Chem.* 85, 1–9.
- Nihemaiti, M., Roux, J.L., Hoppe-Jones, C., Reckhow, D.A., Croue, J.-P., 2017. Formation of haloacetonitriles, haloacetamides, and nitrogenous heterocyclic byproducts by chloramination of phenolic compounds. *Environ. Sci. Technol.* 51, 655–663.
- Pagsberg, P.B., 1972. Investigation of the NH_2 radical produced by pulse radiolysis of ammonia in aqueous solution. *Riso Report* 256, 209–221.
- Pressley, T.A., Bishop, D.F., Roan, S.G., 1972. Ammonia-nitrogen removal by breakpoint chlorination. *Environ. Sci. Technol.* 6, 622–628.
- Rahn, R.O., Bolton, J., Stefan, M.I., 2006. The iodide/iodate actinometer in UV disinfection: determination of the fluence rate distribution in UV reactors. *Photochem. Photobiol.* 82, 611–615.
- Richardson, S.D., Plewa, M.J., Wagner, E.D., Demarini, D.M., 2007. Occurrence, genotoxicity, and carcinogenicity of regulated and emerging disinfection by-products in drinking water: a review and roadmap for research. *Mutat. Res.* 636, 178–242.
- Ruan, X., Zhang, X., Lei, Y., Lei, X., Wang, C., Yang, X., 2021. UV254 irradiation of N-chloro- α -amino acids: Kinetics, mechanisms, and N-DBP formation potentials. *Water Res.* 199, 117204.
- Shah, A.D., Mitch, W.A., 2011. Halonitroalkanes, halonitriles, haloamides, and N-nitrosamines: a critical review of nitrogenous disinfection byproduct formation pathways. *Environ. Sci. Technol.* 46, 119–131.
- Valentine, R.L., Brandt, K.L., Jafvert, C.T., 1986. A spectrophotometric study of the formation of an unidentified monochloramine decomposition product. *Water Res.* 20, 1067–1074.
- Varanasi, L., Coscarelli, E., Khaksari, M., Mazzoleni, L.R., Minakata, D., 2018. Transformations of dissolved organic matter induced by UV photolysis, Hydroxyl radicals, chlorine radicals, and sulfate radicals in aqueous-phase UV-based advanced oxidation processes. *Water Res.* 135, 22–30.
- Villanueva, C.M., Kogevinas, M., Cordier, S., Templeton, M.R., Vermeulen, R., Nuckols, J.R., Nieuwenhuijsen, M.J., Levallois, P., 2014. Assessing exposure and health consequences of chemicals in drinking water: current state of knowledge and research needs. *Environ. Health Persp.* 122, 213–321.
- Wagner, E.D., Plewa, M.J., 2017. Cho cell cytotoxicity and genotoxicity analyses of disinfection by-products: An updated review. *J. Environ. Sci-China* 58, 64–76.
- Wang, D., Bolton, J.R., Andrews, S.A., Hofmann, R., 2015. Formation of disinfection by-products in the ultraviolet/chlorine advanced oxidation process. *Sci. Total Environ.* 518–519, 49–57.
- Wang, Y., Couet, M., Gutierrez, L., Allard, S., Croué, J.-P., 2020. Impact of DOM source and character on the degradation of primidone by UV/chlorine: reaction kinetics and disinfection by-product formation. *Water Res.* 172, 115463.
- Wang, C., Moore, N., Bircher, K., Andrews, S., Hofmann, R., 2019. Full-scale comparison of UV/H₂O₂ and UV/Cl₂ advanced oxidation: The degradation of micropollutant surrogates and the formation of disinfection byproducts. *Water Res.* 161, 448–458.
- Wang, W.L., Zhang, X., Wu, Q.Y., Du, Y., Hu, H.Y., 2017. Degradation of natural organic matter by UV/chlorine oxidation: molecular decomposition, formation of oxidation byproducts and cytotoxicity. *Water Res.* 124, 251–258.
- Westerhoff, P., Chao, P., Mash, H., 2004. Reactivity of natural organic matter with aqueous chlorine and bromine. *Water Res.* 38, 1502–1513.
- Wols, B.A., Hofman-Caris, C.H., 2012. Review of photochemical reaction constants of organic micropollutants required for UV advanced oxidation processes in water. *Water Res.* 46, 2815–2827.
- Wu, Z., Guo, K., Fang, J., Yang, X., Xiao, H., Hou, S., Kong, X., Shang, C., Yang, X., Meng, F., 2017. Factors affecting the roles of reactive species in the degradation of micropollutants by the UV/chlorine process. *Water Res.* 126, 351–360.
- Wu, Q.Y., Zhou, Y.T., Li, W., Zhang, X., Du, Y., Hu, H.Y., 2019a. Underestimated risk from ozonation of wastewater containing bromide: Both organic byproducts and bromate contributed to the toxicity increase. *Water Res.* 162, 43–52.
- Wu, Y., Zhu, S., Zhang, W., Bu, L., Zhou, S., 2019b. Comparison of diatrizoate degradation by UV/chlorine and UV/chloramine processes: Kinetic mechanisms and iodinated disinfection byproducts formation. *Chem. Eng. J.* 375, 121972–121981.
- Yang, X., Fan, C., Shang, C., Zhao, Q., 2010. Nitrogenous disinfection byproducts formation and nitrogen origin exploration during chloramination of nitrogenous organic compounds. *Water Res.* 44, 2691–2702.
- Yang, X., Shang, C., Lee, W., Westerhoff, P., Fan, C., 2008. Correlations between organic matter properties and DBP formation during chloramination. *Water Res.* 42, 2329–2339.
- Yeom, Y., Han, J., Zhang, X., Shang, C., Zhang, T., Li, X., Duan, X., Dionysiou, D.D., 2021. A review on the degradation efficiency, DBP formation, and toxicity variation in the UV/chlorine treatment of micropollutants. *Chem. Eng. J.* 424, 130053.

- Yin, R., E.R. Blatchley, I.I.I., Shang, C., 2020. Uv photolysis of mono- and dichloramine using UV-LEDs as radiation sources: photodecay rates and radical concentrations. *Environ. Sci. Technol.* 54, 8420–8429.
- Zhang, X., He, J., Xiao, S., Yang, X., 2019a. Elimination kinetics and detoxification mechanisms of microcystin-LR during UV/chlorine process. *Chemosphere* 214, 702–709.
- Zhang, X., Li, W., E.R. Blatchley, I.I.I., Wang, X., Ren, P., 2015. UV/chlorine process for ammonia removal and disinfection by-product reduction: Comparison with chlorination. *Water Res.* 68, 804–811.
- Zhang, D., Li, W., Huang, X., Qin, W., Liu, M., 2013. Removal of ammonium in surface water at low temperature by a newly isolated microbacterium sp. strain SFA13. *Bioresour. Technol.* 137, 147–152.
- Zhang, X., Ren, P., Li, W., Lei, Y., Yang, X., Blatchley, E.R., 2019b. Synergistic removal of ammonium by monochloramine photolysis. *Water Res.* 152, 226–233.
- Zhou, S., Wu, Y., Zhu, S., Sun, J., Bu, L., Dionysiou, D.D., 2020. Nitrogen conversion from ammonia to trichloronitromethane: Potential risk during UV/chlorine process. *Water Res.* 172, 115508.
- Zi, Y., Liu, W.J., Sun, W.J., Nie, X.B., Ao, X.W., 2018. Role of ammonia on haloacetonitriles and halonitromethanes formation during ultraviolet irradiation followed by chlorination/chloramination. *Chem. Eng. J.* 337, 275–281.